Inorganica Chimica Acta 464 (2017) 186–194

Contents lists available at ScienceDirect

Inorganica Chimica Acta

journal homepage: www.elsevier.com/locate/ica

Research paper

Copper(II)-salicylaldehydate/-methoxy(pyridine-2-yl)methanolate complexes *via* in-situ hydrolysis of Schiff bases

Mohammed Enamullah [a,*], Anne-Christine Chamayou [b], Kazi Saima Banu [a], Anna Christin Kautz [b], Christoph Janiak [b,*]

[a] Department of Chemistry, Jahangirnagar University, Dhaka 1342, Bangladesh
[b] Institut für Anorganische Chemie und Strukturchemie, Heinrich-Heine-Universität, Universitätsstr. 1, D-40225 Düsseldorf, Germany

ARTICLE INFO

Article history:
Received 11 March 2017
Received in revised form 25 April 2017
Accepted 1 May 2017
Available online 5 May 2017

Keywords:
Cu(II)-salicylaldehydate/-methoxy (pyridine-2-yl)methanolate
Mixed-ligated dinuclear copper(II)-complexes
In-situ hydrolysis of the Schiff base ligands
Cyclic voltammograms
DFT/TDDFT

ABSTRACT

Reaction of copper(II) nitrate with N-2-(R-pyridyl)salicylaldimine affords the mononuclear *bis*[salicylaldehydato-κO,O′]copper(II) (**1**) *via* acidic hydrolysis of the aldimine ligand back to the salicylaldehyde. Similarly, reaction with (*R*)-N-1-(*p*-BrC_6H_4)ethyl-salicylaldimine or (*R*)-1-(*p*-BrC_6H_4)-N-((pyridin-2-yl) methylene)ethanamine in presence of 2,2′-bipyridine (bipy) provides the mixed-ligated dinuclear *bis* [(μ-salicylaldehydato-κO,O′:O′)(2,2′-bipyridine)nitrato-copper(II)] (**2**) or *bis*[{μ-methoxy(pyridine-2-yl) methanolato-κN,O:O}(methanol)nitrato-copper(II)] (**3**). The structures of **2** and **3** consist of a dinuclear unit involving two (bipy)(salicylaldehydate)- or {methoxy(pyridine-2-yl)methanolate}(methanol)-coordinated copper(II) cations and two nitrate anions. The coordination sphere of copper is of N2O4-type with an elongated octahedron due to the Jahn-Teller effect in **2**. The axial positions of the square bipyramid are occupied by the oxygen atoms from NO_3^- and the phenoxo group of the nearest salicylaldehydate molecule. The coordination sphere of copper is of NO4-type in **3**, with the alkoxido group of methoxy (pyridine-2-yl)methanolate bridging between the Cu atoms. Cyclic voltammograms for **1** demonstrate two quasi-reversible one electron charge transfer processes for $[Cu(L)_2]^{2-}/[Cu(L)_2]^-$ and $[Cu(L)_2]^-/[Cu(L)_2]$ (L = salicylaldehydato), respectively in acetonitrile. DSC analyses reveal an irreversible phase transformation from solid to solid-liquid mixture phase, and then to an isotropic liquid phase for **1**. The excited state properties of **1** studied by DFT/TDDFT are comparable to the experimental electronic spectrum.

© 2017 Elsevier B.V. All rights reserved.

1. Introduction

Syntheses and characterization of transition metal(II)-N-2-(*R*-pyridyl)-salicylaldimine complexes are of continued interests due to their electrochemical, thermal, molecular magnetism, and supramolecular properties as well as X-ray molecular structures with variable coordination geometry [1–3]. The ligands coordinate to the metal ion *via* phenolic-O and imine-N atoms in tetrahedral to square-planar geometry, and provide the mononuclear complexes $[Cu(N\text{^}O)_2]$ {N^O⁻ = N-2-(R-pyridyl)salicylaldiminato} [2a,b]. Though the pyridyl *N*-atom is not involved in metal co-ordination sphere, it participates in an intramolecular hydrogen bonding with the imine-H atom [2a]. In addition, the π–π stacking between the benzene rings and the pyridyl rings links the molecules into a supramolecular one-dimensional chain. We have recently given attentions to syntheses, spectroscopy, thermal and magnetic properties, cyclic voltammetry, and molecular structures of transition metal(II)-chiral Schiff base complexes of mononuclear non-planar $[M(R/S\text{-}N\text{^}O)_2]$ (M = Cu/Ni/Zn(II), N^O⁻ = (*R*/*S*)-N-1-(Ar)ethyl-salicylaldiminato or -naphthaldiminato) [4–9] and mixed-ligated Rh(η^4-cod)(*R*/*S*-N^O) [10–15]. Molecular structures typically show *bis*-N^O-chelation of the Schiff base ligands to the metal(II) ion with a N2O2-chromophore in four coordinated distorted tetrahedral (Zn) to square-planar (Cu/Ni) geometry. Such complexes are readily obtained by reactions of Cu/Zn(II) salts and Schiff-base ligands. We have further reported the similar Cu/Zn(II)-complexes with N-2-(*R*-pyridyl)-salicylaldimine/-naphthaldimine [16–18].

It is well documented that the synthesis of a Schiff base from aldehyde and amine is a reversible process, and hydrolysis of the Schiff base due to more or less small amounts of water will regenerate the original aldehyde (see Scheme 1) [19,20]. Hence, reactions between copper(II) nitrate and N-2-(R-pyridyl)-salicylaldimine {R = H (HL1), 4/6-CH_3 (HL2/HL3)} provided dark brown block shaped crystals of the known compound *bis*[salicylaldehydato-κO,O′]copper(II) (**1**), where the regenerated salicylaldehyde

* Corresponding authors.
E-mail addresses: enamullah@juniv.edu (M. Enamullah), janiak@uni-duesseldorf.de (C. Janiak).

http://dx.doi.org/10.1016/j.ica.2017.05.001
0020-1693/© 2017 Elsevier B.V. All rights reserved.

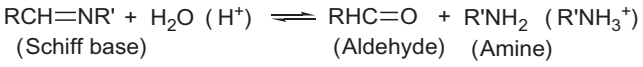

Scheme 1. Equilibrium of Schiff base formation and hydrolysis.

coordinates to the copper(II) as a deprotonated salicylaldehydato ligand (Scheme 2) [20,21].

Similarly reactions between copper(II) nitrate and the chiral Schiff base ligand, (*R*)-N-1-(*p*-BrC_6H_4)ethyl-salicylaldimine (HL4) or (*R*)-1-(*p*-BrC_6H_4)-N-((pyridin-2-yl)methylene)ethanamine (HL5) in the presence of 2,2′-bipyridine (bipy) provide the mixed-ligated dinuclear green crystals of *bis*[(bipy)(μ-salicylaldehydato-κO,O′:O′)nitrato-copper(II)] (**2**) or *bis*[{μ-methoxy(pyridine-2-yl)methanolato-κN,O:O}(methanol)nitrato-copper(II)] (**3**) (Scheme 3) *via* hydrolysis of the Schiff base ligands. The present paper reports the results of syntheses, spectroscopy, cyclic voltammograms, thermal analyses and X-ray molecular structures of compounds **1**, **2** and **3**, respectively. Further, the excited state UV/Vis absorption spectral properties for **1** are analyzed by DFT/TDDFT, and compared with the experimental results.

2. Experimental

2.1. Materials and measurements

FT-IR spectra were recorded on a Nicolet iS10 (Thermo Scientific) spectrometer as KBr discs at ambient temperature. UV–Vis spectra were obtained with Shimadzu UV 1800 spectrophotometer in chloroform at 25 °C. Differential scanning calorimeter (DSC) analyses were performed on a Shimadzu DSC-60 at the range of 30–230 °C (i. e., up to the decomposition temperature) with a rate of 10 K min^{-1}. An Epsilon™ Instruments (BASi) electrochemical analyzer was used for cyclic voltammetry experiments in acetonitrile containing tetra-*N*-butyl-ammonium-hexaflorophosphate (TBAP) as supporting electrolyte. The three-electrode measurement was carried out at 25 °C with a platinum disc working electrode, a platinum wire auxiliary electrode and a Ag/AgCl reference electrode. The solution containing the copper(II)-complex and TBAP was deoxygenated for 10 min with nitrogen gas prior to use. Elemental analyses were performed on a VarioEL from Elementar. ESI-MS (positive mode) spectra were taken on a Shimadzu LCMS-2020. Isotopic distributions patterns for the $^{63/65}Cu$ containing ions are clearly visible in the mass spectra. Syntheses of the Schiff base ligands N-2-(R-pyridyl)salicylaldimine {R = H (HL1), 4/6-CH_3 (HL2/HL3)}, (*R*)-N-1-(Ar)ethyl-salicylaldimine (HL4) and (*R*)-1-(Ar)-N-((pyridin-2-yl)methylene)ethanamine (HL5) (Ar = *p*-BrC_6H_4) were reported in our previous communications [10–12,16].

2.2. Syntheses of *bis*[salicylaldehydato-κO,O′]copper(II) (**1**)

Two equivalents of N-2-(pyridyl)-salicylaldimine (HL1: 397 mg, 2.00 mmol) dissolved in 10 mL methanol was added into 10 mL hot methanol solution of $Cu(NO_3)_2{\cdot}4H_2O$ (260 mg, 1.00 mmol). The solution was stirred for about 5–6 h at room temperature. The color changed from light green to deep green, and finally to greenish brown. The volume of the solvent was reduced to *ca.* 50% *in vacuo*, and this concentrated solution (greenish brown color) was left standing for crystallization *via* slow evaporation of solvent at room temperature. Dark brown block shaped crystals of *bis*[salicylaldehydato-κO,O′]copper(II) (**1**) (see Fig. S1), suitable for X-ray measurements, were formed after 5–6 days, which were manually separated by a spatula. The crystals were washed with two portions of methanol (2 mL), and dried in air. The same procedure was employed using the Schiff bases N-2-(R-pyridyl)salicylaldimine (R = 4/6-CH_3: HL2/HL3), respectively, and gave the identical dark brown block shaped crystals of **1**, as evidenced by different analytical methods and X-ray analyses (discussed below).

2.2.1. Analysis of compound ***1*** using HL1

Yield: 350 mg (76%). – IR (KBr, cm^{-1}): 3049, 3011, 2911w (H–C), 1610, 1596vs, (C=O), and 1527 s (C=C). – $C_{14}H_{10}O_4Cu$ (305.77): calcd. C, 55.00; H, 3.30 found C 55.64, H 3.35.

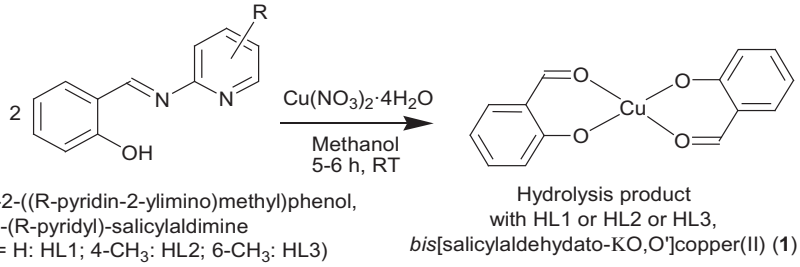

Scheme 2. Synthetic route to the formation of hydrolysed product *bis*[salicylaldehydato-κO,O′]copper(II) (**1**).

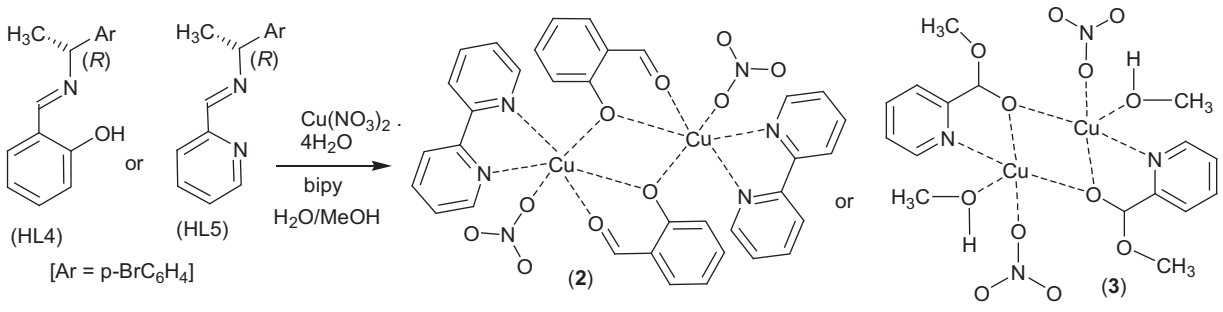

Scheme 3. Synthesis of *bis*[(μ-salicylaldehydato-κO,O′:O′)(bipy)nitrato-copper(II)] (**2**) and *bis*[{μ-methoxy(pyridine-2-yl)methanolato-κN,O:O}(methanol)nitrato-copper(II)] (**3**).

*2.2.2. Analysis of compound **1** using HL2*

Yield: 360 mg (74%). – IR (KBr, cm^{-1}): 3052, 3020, 2923w (H–C), 1610, 1596vs (C=O), and 1527s (C=C). – MS (ESI+): *m/z* = 593/595 $[M_2-OH]^+$, 320/322 $[MO\text{-}H]^+$, 213 $[HL2+H]^+$, 137/139 $[CuO(CHO)_2]^+$ and 109 $[C_6H_5CH_2OH+H]^+$ (M = $C_{14}H_{10}O_4Cu$; Isotopic distribution pattern for $^{63/65}Cu$ containing ions are clearly visible following the peaks at 593, 320 and 137, respectively). – $C_{14}H_{10}O_4Cu$ (305.77): calcd. C, 55.00; H 3.30 found C 55.25, H 3.51.

*2.2.3. Analysis of compound **1** using HL3*

Yield: 350 mg (72%). – IR (KBr, cm^{-1}): 3049, 3019, 2920w (H–C), 1610, 1596vs (C=O), and 1527 s (C=C). – $C_{14}H_{10}O_4Cu$ (305.77): calcd. C, 55.00; H, 3.30 found C 55.73, H 3.39.

*2.3. Synthesis of bis[(μ-salicylaldehydato-κO,O′:O′)(bipy)nitrato-copper(II)] (**2**)*

An equimolar amount of $Cu(NO_3)_2{\cdot}4H_2O$ (130 mg, 0.5 mmol) and (*R*)-N-1-(*p*-BrC_6H_5)ethyl-salicylaldimine (HL4) (152 mg, 0.5 mmol) was dissolved in 5 mL of water/methanol (50%, v/v). NEt_3 was added (70 μL, 0.5 mmol) into this solution, and pH was recorded at 6.0. This solution mixture was refluxed at 90 °C for 1 h. Afterwards, 2,2′-bipyridine (bipy) (79 mg, 0.5 mmol) dissolved in 5 mL methanol was added into the warm solution mixture. The resulting dark green solution was allowed to stand for two days with slow solvent evaporation at room temperature to give green crystals of compound **2** (see Fig. S1). The crystals were collected by suction filtration, washed with a small portion of water and dried in air.

Yield: 116 mg (57%). – IR (KBr, cm^{-1}): 3055 (C–H), 1611 (C=O/N), 1525 (C–C), and 1384, 1314 (NO_3). (ATR, cm^{-1}): 3077w (C–H), 1601, 1572vs (C=O/N), 1532m (C–C) and 1396, 1313 (NO_3). – $C_{34}H_{26}Cu_2N_6O_{10}$ (805.67): C, 50.69, H, 3.25; N, 10.43 Found C 50.55, H 3.31, N 10.44.

Alternative method

$Cu(NO_3)_2{\cdot}4H_2O$ (130 mg, 0.5 mmol) was dissolved in 5 mL of methanol and mixed with HL4 (152 mg, 0.5 mmol) in 5 mL of methanol, and the solution refluxed for 10 min. Then 5 mL of a methanolic solution of bipy (79 mg, 0.5 mmol) was added into this reaction mixture, and continued to stir for 1 h. The solution was filtered and the resulting clear greenish solution was set aside for slow solvent evaporation at room temperature until crystals formed after a few days. The crystals were collected by filtration and dried in air.

Yield: 96 mg (48%). IR (KBr, cm^{-1}): 3034w (C–H), 1605vs (C=O/N), 1523m (C–C) and 1384, 1314 (NO_3). – $C_{34}H_{26}Cu_2N_6O_{10}$ (805.67): C, 50.69; H, 3.25; N, 10.43 found C 51.26, H 3.57, N 10.41.

*2.4. Synthesis of bis[{μ-methoxy(pyridine-2-yl)methanolato-κN,O:O}(methanol)nitrato-copper(II)] (**3**)*

An equimolar amount of $Cu(NO_3)_2{\cdot}4H_2O$ (130 mg, 0.5 mmol) and (*R*)-1-(*p*-BrC_6H_4)-N-((pyridin-2-yl)methylene)ethanamine (HL5) (145 mg, 0.5 mmol) were dissolved in 10 mL of water/methanol (50%, v/v). The solution was heated to reflux for 10 min. Then 5 mL of a methanolic solution of bipy (79 mg, 0.5 mmol) was added into this reaction mixture, and continued to stir for 1 h. The resulting dark green solution was allowed to stand for 2–3 days with slow solvent evaporation at room temperature to give green crystals of compound **3** (see Fig. S1). The crystals were collected by suction filtration, washed with a small portion of water and dried in air.

Yield: 62 mg (21%). – $C_{16}H_{24}O_{12}N_4Cu_2$ (591.44): C, 32.49; H, 4.09; N, 9.47 found C 32.69, H 4.15, N 9.17.

2.5. X-ray structure determination

Single crystals of **1** (from HL2 and HL3), **2** and **3** were mounted in silicon oil on top of glass capillaries or polyimide MicroMounts

Table 1
Crystal data and structure refinement for compounds **1**, **2** and **3**.

Compounds	**1** (from HL2)	**1** (from HL3)	**2**	**3**
Empirical formula	$C_{14}H_{10}CuO_4$	$C_{14}H_{10}CuO_4$	$C_{34}H_{26}Cu_2N_6O_{10}$	$C_{16}H_{24}Cu_2N_4O_{12}$
M/g mol^{-1}	305.76	305.76	805.71	591.49
Crystal size/mm	0.25 × 0.18 × 0.01	0.80 × 0.37 × 0.07	0.22 × 0.12 × 0.03	0.38 × 0.28 × 0.10
2θ range/°	5.4–55.00	4.8–55.00	4.22–54.00	4.50–56.00
h; *k*; *l*; range	±11; ±8; ±14	±11; ±8; ±14	±10; ±12; −12, 13	±9; ±11; ±13
Crystal system	monoclinic	monoclinic	triclinic	triclinic
Space group	$P2_1/n$	$P2_1/n$	$P-1$	$P-1$
a/Å	8.6921(4)	8.7091(9)	8.3936(17)	7.4711(2)
b/Å	6.2186(3)	6.2176(6)	9.847(2)	8.9273(2)
c/Å	11.2034(5)	11.2198(11)	10.621(2)	9.9496(3)
α/°	90	90	97.61(3)	113.1740(10)
β/°	104.686(2)	104.916(4)	112.40(3)	92.0240(10)
γ/°	90	90	96.66(3)	101.8310(10)
V/Å^3	585.79(5)	587.08(10)	791.1(3)	592.12(3)
Z	2	2	2	1
D_{calc}/g cm^{-3}	1.733	1.730	1.691	1.659
F (000)	310	310	410	302
μ/mm^{-1}	1.870	1.866	1.417	1.862
Max/min transmission	0.7456/0.6336	0.7456/0.5311	0.9547/0.7410	0.8429/0.5411
Reflect. collected (R_{int})	10,081 (0.0217)	10,141 (0.0262)	9991 (0.0178)	19,695 (0.0229)
Independ. reflections	1339	1339	3451	2847
Obs. reflect. [$I > 2\sigma(I)$]	1285	1286	3129	2724
Parameters refined	88	88	235	159
Max./min. $\Delta\rho$[a]/e Å^{-3}	0.526/−0.308	0.455/−0.306	0.588/−0.295	0.689/−0.286
R_1/wR_2 [$I > 2\sigma(I)$][b]	0.0231/0.0757	0.0243/0.0771	0.0271/0.0722	0.0223/0.0642
R_1/wR_2 (all reflect.)[b]	0.0238/0.0753	0.0250/0.0766	0.0310/0.0740	0.0238/0.0652
Goodness-of-fit on F^2[c]	1.145	1.147	1.067	1.064
Weight. scheme *w*; *a*/*b*[d]	0.0451/0.3268	0.0450/0.3367	0.0413/0.2968	0.0371/0.3094

[a] Largest difference peak and hole.
[b] $R_1 = [\Sigma(||F_o| - |F_c||)/\Sigma|F_o|]$; $wR_2 = [\Sigma[w(F_o^2 - F_c^2)^2]/\Sigma[w(F_o^2)^2]]^{1/2}$.
[c] Goodness-of-fit = $[\Sigma[w(F_o^2 - F_c^2)^2]/(n-p)]^{1/2}$.
[d] $w = 1/[\sigma^2(F_o^2) + (aP)^2 + bP]$ where $P = (\max(F_o^2 \text{ or } 0) + 2F_c^2)/3$.

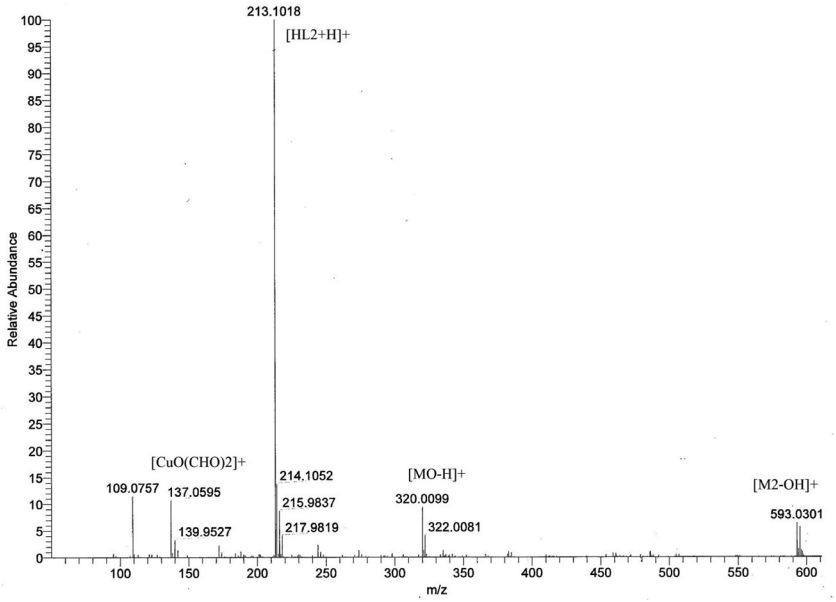

Fig. 1. ESI-mass spectra for compound **1** (from HL2).

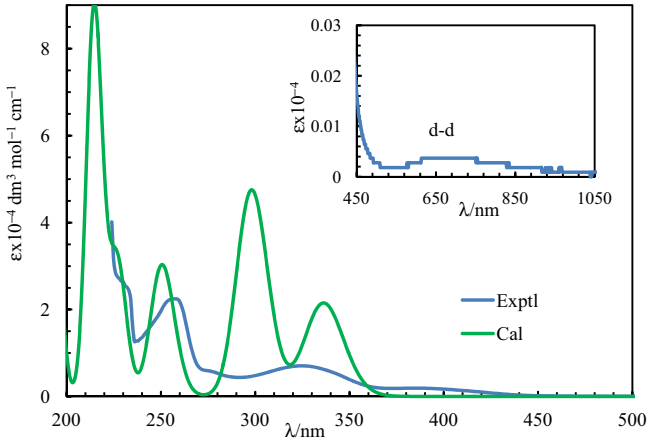

Fig. 2. Experimental (0.22 mmol dm^{-3}) and computed (cam-b3lyp/tzvp//b3lyp/6-31g(d)) electronic spectra for **1** (from HL2) in chloroform at 25 °C (inset: units of ε is $dm^3\ mol^{-1}\ cm^{-1}$).

(supplied by MiTeGen). Data were collected on a Bruker Kappa APEX-II CCD area detector Diffractometer [22] using sealed-tube Mo-K_α radiation. During measurements, the crystals were cooled with a Bruker Cryopad at 150 K for **1**, and at 203 K for **2** and **3**. Unit cell parameters strategies were calculated from a least-squares refinement of at least 1000 collected reflections. Structures were solved by direct methods in the SHELXS-97 [23] program. Successive interpretation of the difference Fourier maps and refinement against F^2 was carried out with the SHELX-97 program suite [23]. All non-hydrogen atoms were assigned anisotropic parameters during the refinement. Hydrogen atoms were included at calculated positions and refined isotropically based on a riding model (AFIX 43 for aromatic H atoms). Occasionally, atomic movement in the anions was restricted with SADI, DFIX constraints. The crystal data and details on the structure refinement are given in Table 1.

2.6. Computational method

Computation was carried out with the Gaussian 09 software package [24]. For computation, the initial geometry was generated from the X-ray structure for **1** (from HL2). The gas phase equilibrium geometry was optimized with DFT using b3lyp functional with 6-31g(d) basis set. The absence of any imaginary frequencies confirmed that the stationary points correspond to minima on the Potential Energy Surface. For computation, time-dependent density functional theory (TDDFT) was employed with the cam-b3lyp or m06 functionals and the basis sets tzvp on the optimized structure, incorporating PCM (Polarization Continuum Model) using chloroform as a solvent. For TDDFT calculations, 72 excitation states were considered (Table S2). For assignments of excited state properties, the molecular orbital (MO) calculations were performed using same level of theory. The computed electronic spectrum was compared with the experimental one, and the best fit was observed with b3lyp/tzvp//b3lyp/6-31g(d) calculations.

3. Results and discussion

3.1. Syntheses, spectroscopic and structural analyses for compound *1*

Reaction of N-2-(R-pyridyl)salicylaldimine {R = H (HL1) or 4-CH_3 (HL2) or 6-CH_3 (HL3)} with copper(II) nitrate in methanol (not dried) provides the *bis*[salicylaldehydato-κO,O′]copper(II) (**1**) (Scheme 2) *via* hydrolysis of the Schiff base back to the salicylaldehyde. Hydrolysis of N-2-(R-pyridyl)salicylaldimine induced by Cu(acetate)$_2$·H_2O (i. e., metal-induced hydrolytic cleavage of the imine-bond during slow crystal growth) in dichloromethane/methanol provided the same compound **1** [21e]. In fact, the free ligands such as N-2-(R-pyridyl)salicylaldimine and N-*o*-Vanillylidene-L-histidine also undergo hydrolysis with more or less small amounts of water in the reaction mixture [19,20]. However, compound **1** can also be synthesized from direct reaction between salicylaldehyde and Cu(acetate)$_2$·H_2O in acetonitrile/methanol [21d]. Most likely it is the water content and not the solvent or presence of Cu^{2+} which induces the hydrolysis as long as the solvent dissolves all reaction partners. In an earlier study on the Schiff base compound N-*o*-vanillylidene-L-histidine we had studied the imine bond hydrolysis by ^{1}H NMR spectroscopy which revealed that N-*o*-vanillylidene-L-histidine is quickly hydrolysed and in equilibrium with *o*-vanillin and L-histidine in aqueous solution [19]. Elemental data show the absence of any

Table 2
Excitation properties for compound **1** (from HL2), calculated by cam-b3lyp/tzvp//b3lyp/6-31g(d) in chloroform.[#]

λ/nm[a]	Oscillator Strength (f)	MOs contributions (%)[b]	Assignments[c]
380 (385)	0.0001	H-2→L + 2 (34)	d-d, ML
336 (325)	0.2123	H-1→L + 1 (36), H→L + 2 (56)	d-d, ML, LL
299 (270sh)	0.4038	H-4→L (157)	d-d, ML
249 (258)	0.1876	H-7→L (47), H-3→L + 1 (23)	d-d, ML, LL
227 (229)	0.2299	H-7→L (97), H→L + 6 (13)	d-d, ML, LL
215	0.7229	H→L + 4 (39)	d-d, ML, LL

[#] β-spin MOs are considered.
[a] Experimental bands are (concentration of solution: 0.22 mmol dm^{-3}) in parentheses.
[b] H = HOMO and L = LUMO.
[c] d-d = metal-centred, ML = metal-ligand and LL = ligand-centred transitions.

nitrogen in all three batches of compounds, strong indication in favor of formation of salicylaldehyde, and subsequent formation of compound **1**. The experimental results (i. e., elemental, DSC, cyclic voltammetry and mass data) are the same for the compounds obtained from three batches using the three starting ligands HL1, HL2 and HL3, respectively (see experimental section). Vibrational spectra show the strong bands/shoulders at 1610/1596 and 1527 cm^{-1}, associated to *ν*C=O and *ν*C=C, respectively. Several weak bands are found at 3050–2910 cm^{-1}, due to *ν*C–H. ESI-MS spectrum for **1** (Fig. 1) shows the ion peaks at *m*/*z* 593 for $[M_2-OH]^+$ and 320 for $[M+O-H]^+$, supporting the formation of compound **1**. Noteworthy, no peaks are seen which would correspond to the formation of $[Cu(L2)_2]$ {L2 = N-2-(4-methyl-pyridyl) salicylaldiminate} [2a,b,18]. The spectrum further shows the peak for the protonated Schiff base ligand at *m*/*z* 213 $[HL2+H]^+$, and several other peaks for the fragmented compound species, respectively. Single crystal X-ray structure analysis confirms the molecular structure of **1** (Fig. S2) to consist of two O^O-chelates ligands from salicylaldehydates around the copper(II) ion in a square planar geometry. The structure has been reported and discussed before [20,21].

3.1.1. Experimental and computed electronic spectra for *1*

Electronic spectra for the different batches of compound **1** are identical (Fig. 2), and show strong bands/shoulders below 300 nm due to ligand-centered $n\rightarrow\pi^*/\pi\rightarrow\pi^*$ (LLCT) transitions. A moderate broad band at 300–450 nm, assigned to the metal-ligand (MLCT) charge transfer transitions. The spectra further feature a weak broad band at visible region (500–1050 nm) due to the superposition of several metal-centered d-d transitions bands (Fig. 2, inset) [5,8b,17,18]. Spectra taken at different time intervals demonstrate that the compound decomposes very fast at *ca.* 11% within 5 min (*ca.* 34% within 1 h) of dissolution in chloroform, a common feature of square-planar Cu(II)-O^O-chelate complexes in solution (Fig. S3). The LLCT bands become more intense, while MLCT bands disappear with increasing time. In fact, the presences of several isosbestic points at *ca.* 350, 310, 265, and 248 nm (Fig. S3) indicate the existing equilibria among different ionic species resulting from decomposition in solution.

A computational procedure is carried out with the aim to rationalize the experimental electronic spectra in solution. For computation, TDDFT is employed with cam-b3lyp/tzvp//b3lyp/6-31g(d), incorporating PCM (Polarization Continuum Model) using chloroform as a solvent. For comparison, TDDFT is further employed with m06/tzvp//b3lyp/6-31g(d). However, the best fitted computed spectrum to the experimental one is obtained with cam-b3lyp/tzvp//b3lyp/6-31g(d) calculations (Fig. 2). Indeed, a straightforward assignments on computed spectra for open-shell metal complexes are hampered by the complexity of the system (in particular spin contamination), and presences of a large number of transitions at a single excitation state (i.e., at a particular wavelength), as evidenced from the Supporting information (Table S2) [5,17,18,25–27]. Thus we report herein only the selected and simplified assignments relevant to the experimental data in Table 2. However, the assignments are based on the orbital and population analyses. Hence, a combined d-d, ML and/or LL transitions bands appear with absorption maxima at *ca.* 336 nm with the highest molecular orbitals (MOs) contribution of 36% (HOMO − 1 to LUMO + 1) for β-spin consideration. The HOMOs − 1 and LUMOs + 1 for β-spin consideration are presented in Fig. 3. Further, there are also several computed bands which are very close to the observed experimental bands/shoulders within in a little deviation (Fig. 2 and Table 2). In fact, the strongest band at 215 nm in computed spectrum is not seen in experimental one due to solvent's absorption. On the other hand, the d-d band observed in the experimental spectrum at visible range is not detected in the computed one.

3.2. Syntheses and structural analyses for compound *2*

Refluxing copper(II) nitrate with (*R*)-N-1-(*p*-BrC_6H_4)ethyl-salicylaldimine (HL4) in presence of 2,2′-bipyridine (bipy) in water/methanol (50%, v/v) leads to the formation of deep green crystals of *bis*[(μ-salicylaldehydato-κO,O′:O′)(bipy)nitrato-copper(II)] (**2**)

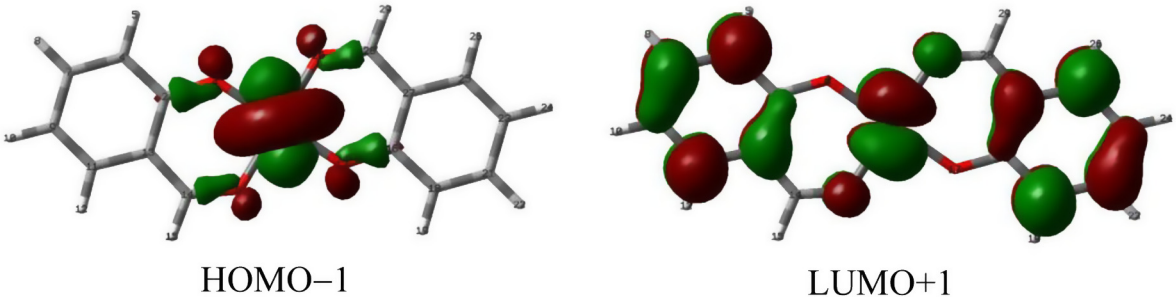

Fig. 3. The HOMOs − 1 and LUMOs + 1 for **1** for β-spin consideration, calculated by cam-b3lyp/tzvp//b3lyp/6-31g(d) in chloroform.

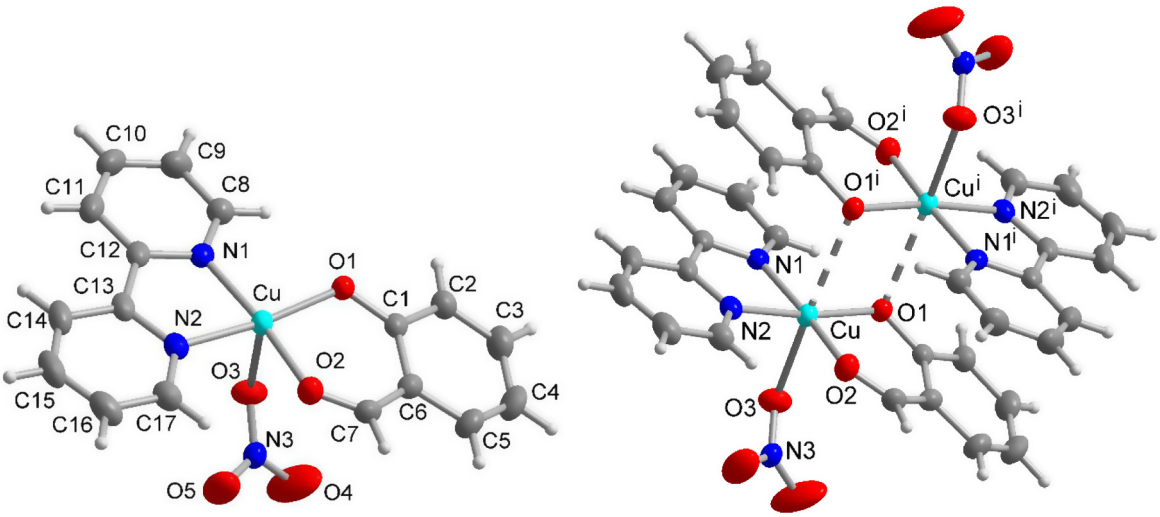

Fig. 4. Molecular structure for compound **2**, as asymmetric unit (left) and as dinuclear/dimeric entity (right) (50% thermal ellipsoids). Symmetry transformation, i = 1 − x, 1 − y, −z. See Table 3 for selected bond distances and angles.

Table 3
Selected bond distances (Å) and angles (°) in compounds **1**, **2** and **3**.

Compound	**1** (from HL2)	**1** (from HL3)	**2**		**3**	
Cu–Cu^{i}	–	–	Cu–Cu^{i}	3.5251(12)	Cu–Cu^{i}	2.9817(3)
Cu–O1	1.8891(11)	1.8891(12)	Cu–O1	1.9162(14)	Cu–O1	1.9276(11)
Cu–O2	1.9423(11)	1.9412(12)	Cu–O2	1.9576(15)	Cu–O3	1.9587(11)
			Cu–N1	1.9952(17)	Cu–O6	2.2836(12)
			Cu–N2	1.9924(17)	Cu–N1	1.9831(14)
			Cu–O1^{i}	2.7060(16)	Cu–O1^{i}	1.9549(12)
			Cu–O3	2.4131(16)		
O1^{i}–Cu–O1	180.00	180.00	O1–Cu–O2	92.83(6)	N1–Cu–O3	98.45(5)
O1–Cu–O2	93.40(5)	93.38(5)	O1–Cu–N2	172.25(6)	O1–Cu–N1	82.36(5)
O1–Cu–O2^{i}	86.60(5)	86.62(5)	O2–Cu–N2	90.87(7)	O1–Cu–O6	98.49(5)
O2^{i}–Cu–O2	180.00(5)	180.00	O1–Cu–N1	94.79(7)	O3–Cu–O6	81.94(5)
			O2–Cu–N1	171.98(6)	N1–Cu–O1^{i}	154.588(52)
			O1–Cu–O1^{i}	82.063(50)	O1–Cu–O1^{i}	79.652(46)
			O1–Cu–O3	88.02(6)		
			O2–Cu–O3	94.92(6)		
			N1–Cu–O3	87.85(6)		
			N2–Cu–O3	98.44(6)		

Symmetry transformation **1**: i = −*x* + 1, −*y* + 2, −*z* + 1; **2**: i = 1 − x, 1 − y, −z; **3**: i = −x, −y, −z.

(Scheme 3). During complexation reaction, the C=N imine bond from Schiff base is hydrolysed back to the salicylaldehyde, which in turn coordinates to the copper(II) ion together with bipy and nitrate to give compound **2**. However, reaction between copper (II) acetate and (*R*/*S*)-N-1-(Ar)ethyl-salicylaldimine or -naphthaldimine in absence of bipy affords the mononuclear [Cu(L)$_2$] (L = deprotonated Schiff base ligand) [5,9].

The molecular structure of **2** consists of a dinuclear unit (Fig. 4) involving two (salicylaldehydato)(bipy)-copper(II) cations and two nitrate anions. The two halves of the dinuclear complex are related by crystallographic centre of symmetry (inversion center) with a Cu···Cu distance of 3.5251(12) Å. The coordination sphere of copper can be described as an elongated six coordinated octahedron due to the Jahn-Teller effect. The coordination sphere of copper ion is of N2O4-type. The basal plane is formed by the two *N*-atoms of the bipy and by the two O-atoms of the chelating salicylaldehydate. The axial positions of the elongated octahedron are occupied by the oxygen atoms from a nitrate anion and a bridging phenoxido group of the salicylaldehydate molecule from the other half of the dimer. The selected bond distances and angles in **2** (Table 3) are comparable with those found in (salicylaldehydato)(bipy)-copper (II) perchlorate [28,29] and *bis*[(μ-O,O′-salicylato)(bipy)-copper (II)] acetylsalicylic acid dehydrate [30], and somewhat higher than the values of the equatorial Cu–N1 and Cu–N2 bonds in analogous dimeric copper(II)-complexes of (3-methoxysalicylaldiminato) (bipy)copper(II) perchlorate {1.983(2) and 1.981(2) Å} and (4-methoxysalicylaldiminato)(bipy)copper(II) perchlorate {1.990(2) and 1.988(3)} [31]. The crystal packing is mainly determined by C–H···O contacts between the O atoms of the nitrate group and the C–H atoms of bipy.

3.3. Syntheses and structural analyses for compound **3**

Refluxing copper(II) nitrate with (*R*)-1-(*p*-BrC_6H_4)-N-((pyridin-2-yl)methylene)ethanamine (HL5) in the presence of 2,2′-bipyridine (bipy) in methanol leads to the formation of green crystals of *bis*[{μ-methoxy(pyridine-2-yl)methanolato-κN,O:O}(methanol) nitrato-copper(II)] (**3**) (Scheme 3). During the reaction, the imine C=N bond from Schiff base (HL5) is hydrolysed back to the amine and picolinaldehyde, which further reacts with methanol to give the hemi-acetal methoxy(pyridine-2-yl)methanol (Scheme 4), and the deprotonated hemi-acetal coordinates to the copper(II) atom to provide the compound **3**. Our attempts to isolate the intact ligand HL5 in its deprotonated form as a copper(II)-bipy complex

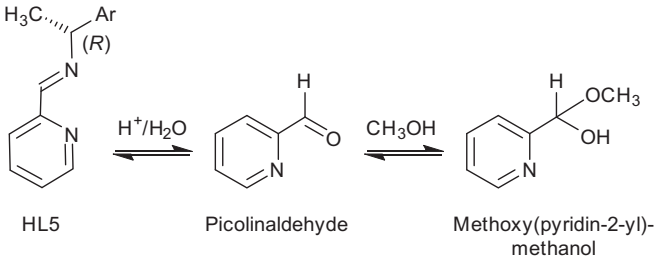

Scheme 4. Conversion of (*R*)-1-(*p*-BrC_6H_4)-N-((pyridin-2-yl)methylene)ethanamine (HL5) into methoxy(pyridin-2-yl)methanol.

{i.e., [Cu(L5)(bipy)]} always led to the isolation of compound **3**, which contains only a fragment of this ligand without bipy as shown in Scheme 2.

The molecular structure of **3** consists of a dinuclear unit (Fig. 5) with two methoxy(pyridine-2-yl)methanolato-copper(II) cations, two nitrate anions and two methanol ligands. The selected bond distances and angles are given in Table 3. The coordination sphere of copper ion is of the NO4-type. Compound **3** is an alkoxido-bridged dinuclear copper(II) complex, where each copper atom is five-coordinated. The asymmetric unit is formed by half a dimer with a chelating methoxy(pyridine-2-yl-κN)methanolate-κO ligand, an anion NO_3^- and a methanol molecule. The two halves of the dinuclear complex are related by crystallographic centre of symmetry (inversion center) with a Cu···Cu distance of 2.9817(3) Å. The oxygen atom of the deprotonated hydroxyl group is simultaneously linked to two metal ions (i.e., bridges between two copper atoms). Hence, the basal plane is formed by the pyridine-N, deprotonated hydroxyl-O, nitrate-O and methanol-O atoms.

3.4. Thermally induced phase transformation for compound *1*

Thermally induced structural phase transformation has been reported for the transition metal(II)-O^O/N^O-chelate complexes, accompanying a change from solid crystalline phase at low temperature (distorted square-planar/tetrahedral) to isotropic liquid phase at high temperature (regular square-planar/tetrahedral geometry) [4–8,16–18]. Differential Scanning Calorimetry (DSC) heating curves for all three batches of compound **1** are identical, and show two exothermic peaks at 230–280 °C (separated by 10–20 °C) with heat of transformation values, ΔH = −33.26 to −31.00 kJ mol^{-1} (Figs. 6, S4). The results correspond to a phase transformation from solid to solid-liquid mixture phase, and then

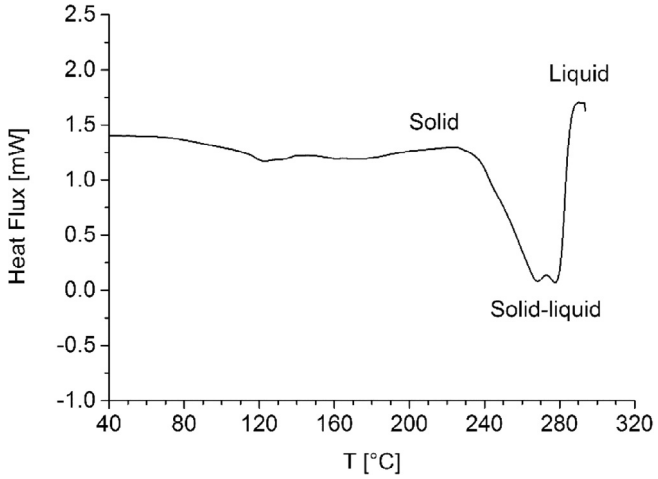

Fig. 6. Differential Scanning Calorimetry (DSC) heating curve for compound **1** (from HL2).

to an isotropic liquid phase. The cooling curves show no corresponding peaks on the reverse direction, suggesting an irreversible phase transformation.

3.5. Cyclic voltammograms for compound *1*

Cyclic voltammograms for compound **1** are recorded at −1.00 to 0.60 V *vs.* Ag/AgCl, using variable switching potentials and scans rates in acetonitrile at 25 °C, respectively (Figs. 7, S5). The reductive response shows a very strong broad cathodic peak (*Ic*) at potential *ca.* −0.70 V (*Ec*), resulting from two electrons charge transfer processes for $[Cu(L)_2]/[Cu(L)_2]^-$ and $[Cu(L)_2]^-/[Cu(L)_2]^{2-}$ (L = salicylaldehydato) couples, respectively. The oxidative response, on the other hand, shows two separate anodic peaks (*Ia*2 & *Ia*1) at potentials *ca.* −0.20 (*Ea*2) and 0.40 V (*Ea*1), corresponds to the first and second electron transfer processes for $[Cu(L)_2]^{2-}/[Cu(L)_2]^-$ and $[Cu(L)_2]^-/[Cu(L)_2]$ couples, respectively. Thus the reversibility of the reductive waves is well illustrated by the presence of corresponding oxidative waves. Analyses of voltammograms with increasing scans rates (v/Vs^{-1}) demonstrate that both the reduction and oxidation peaks become intense, and shift to lower and higher potentials, respectively (Fig. 8, Table S1). Thus, the cathodic peak current (*Ic*) or anodic to cathodic peak current

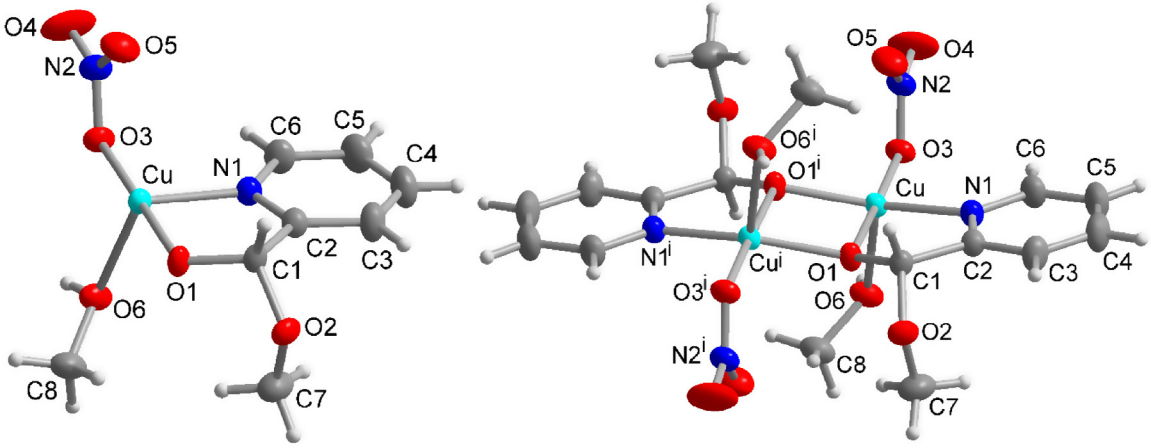

Fig. 5. Molecular structure for **3** as asymmetric unit (left) and as a dinuclear/dimeric entity (right) (50% thermal ellipsoids). Symmetry transformation, i = −x, −y, −z. See Table 3 for selected bond distances and angles.

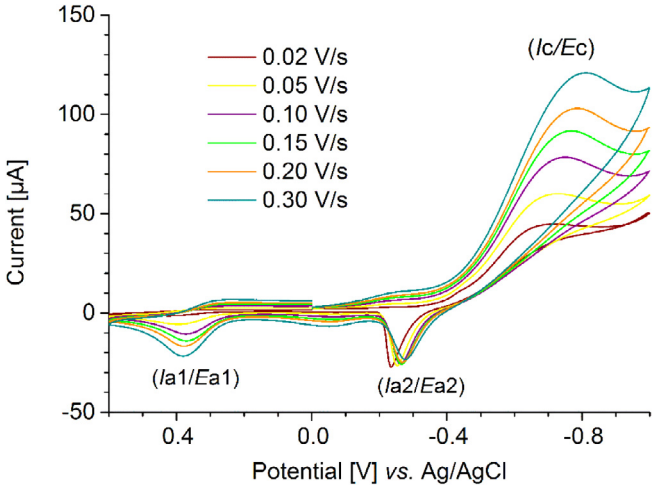

Fig. 7. Cyclic voltammograms for compound **1** (from HL1; 0.5 mmol dm^{-3}) with varying scan rates (v/Vs^{-1}); TBAP (0.1 mol dm^{-3}) in acetonitrile at 25 °C.

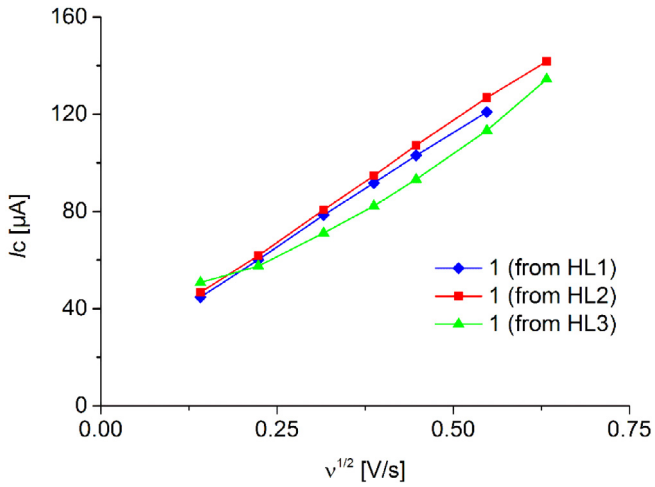

Fig. 8a. Cathodic peak current (*Ic*) *vs.* $v^{1/2}$ [Vs^{-1}] for **1**.

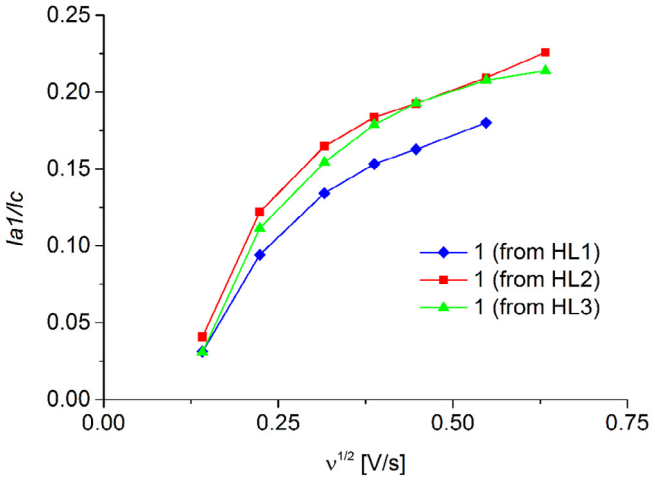

Fig. 8b. Anodic to cathodic peak current ratio (*Ia*1/*Ic*) *vs.* $v^{1/2}$ [Vs^{-1}] for **1**.

ratio (*Ia*1/*Ic*) increases with faster scans rates (Figs. 8a and b), while *Ia*2/*Ic* decreases (Fig. 8c). The overall peaks separation values (ΔEa2 or ΔEa1) remain almost unchanged with varying scans rates

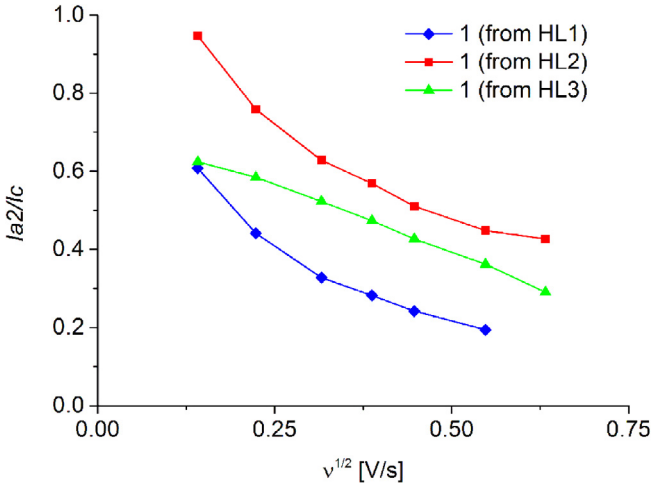

Fig. 8c. Anodic to cathodic peak current ratio (*Ia*2/*Ic*) *vs.* $v^{1/2}$ [Vs^{-1}] for **1**.

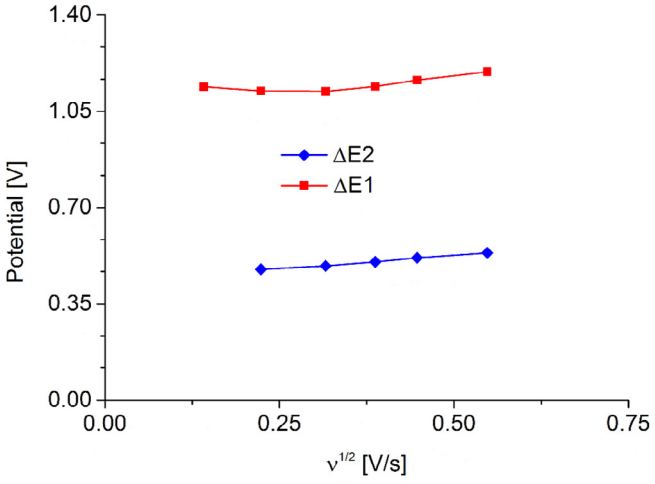

Fig. 8d. Peak separation Δ*E*2 or Δ*E*1 [V] *vs.* $v^{1/2}$ [Vs^{-1}] for **1** (from HL1).

(Fig. 8d). The results are diagnostic for two quasi-reversible one electron charge transfer processes for Cu^{2+}/Cu^{+} and Cu^{+}/Cu couples, respectively [5,17,18,32]. In fact, the observed linear relationships between *Ic* (or *Ia*1 or *Ia*2/*Ic*) and $v^{1/2}$ [Vs^{-1}] represent a diffusion-controlled electrochemical process for **1** in acetonitrile.

4. Conclusions

Reaction of copper(II) nitrate with N-2-(R-pyridyl)salicylaldimine affords the mononuclear *bis*[salicylaldehydato-κO,O′]-copper(II) (**1**) *via* acidic hydrolysis of the ligand to the salicylaldehyde, which is confirmed by re-determination of the single-crystal X-ray structure. Similarly, reaction of copper(II) nitrate with (*R*)-N-1-(*p*-BrC_6H_4)ethyl-salicylaldimine or (*R*)-1-(*p*-BrC_6H_4)-N-((pyridin-2-yl)methylene)ethanamine in the presence of 2,2′-bipyridine leads to hydrolysis of the Schiff base ligands, and provides the mixed-ligated dinuclear *bis*[(μ-salicylaldehydato-κO,O′:O′)(bipy) nitrato-copper(II)] (**2**) or *bis*[{μ-methoxy(pyridine-2-yl)methanolato-κN,O:O}(methanol)nitrato-copper(II)] (**3**). The structures of **2** or **3** consist of dinuclear units involving two (bipy)(salicylaldehydate)- or {methoxy(pyridine-2-yl)methanolate}(methanol)-copper (II) cations and two nitrate anions. The coordination sphere of copper is of N2O4-type with an elongated octahedron in **2**. The axial positions of octahedron are occupied by the oxygen atom from NO_3^- and the bridging phenoxido group. Compound **3** reveals a

NO4-type coordination sphere around the five-coordinated copper atom with a chelating methoxy(pyridine-2-yl-κN)methanolate-κO ligand, NO_3^-, an oxygen atom from a bridging alkoxido-group and a methanol molecule. Both halves of the dinuclear molecular structures of **2** and **3** are related by crystallographic inversion symmetry. Cyclic voltammograms for **1** demonstrate two quasi-reversible one electron charge transfer processes for $[Cu(L)_2]/[CuL)_2]^-$ and $[Cu(L)_2]^-/[Cu(L)_2]^{2-}$ (L = salicylaldehydato) couples, respectively in acetonitrile. The excited state properties calculated by DFT/TDDFT are comparable to the experimental UV–Vis spectrum for **1**. DSC analyses for **1** reveal an irreversible phase transformation from solid to solid-liquid mixture phase, and then to an isotropic liquid phase.

Acknowledgements

We acknowledge Wazed Miah Science Research Centre (WMSRC) at Jahangirnagar University, Bangladesh for obtaining CV and elemental data. Our sincere thanks to Professor D. J. Wilson, Department of Chemistry, York University, Toronto for obtaining the ESI-mass spectra.

Appendix A. Supplementary data

Structural data have been deposited with the Cambridge Crystallographic Data Center; CCDC reference numbers are 1535746 (for **1** from HL2), 1535747 (for **1** from HL3), 1535748 (for **2**), and 1535749 (for **3**). These data can be obtained free of charge from The Cambridge Crystallographic Data Centre via www.ccdc.cam.ac.uk/data_request/cif.

Supplementary data associated with this article can be found, in the online version, at http://dx.doi.org/10.1016/j.ica.2017.05.001.

References

[1] (a) J. Drummond, J.S. Wood, J. Chem. Soc., Dalton Trans. (1972) 365;
(b) S. Giri, S. Biswas, M.G.B. Drew, A. Ghosh, S.K. Saha, Inorg. Chim. Acta 368 (2011) 152;
(c) F. Robert, B. Tinant, R. Clérac, P.-L. Jacquemin, Y. Garcia, Polyhedron 29 (2010) 2739;
(d) C. Maxim, T.D. Pasatoiu, V. Ch Kravtsov, S. Shova, C.A. Muryn, R.E.P. Winpenny, F. Tuna, M. Andruh, Inorg. Chim. Acta 361 (2008) 3903;
(e) A. Castineiras, W. Hiller, J. Straehle, J. Romero, R. Bastida, A. Sousa, Acta Crystallogr. C46 (1990) 770;
(f) N.M. Atherton, D.E. Fenton, G.J. Hewson, C.H. McLean, R. Bastida, J. Romero, A. Sousa, E.E. Castellano, J. Chem. Soc., Dalton Trans. (1988) 1059.
[2] (a) J. Miao, Z. Zhao, H. Chen, D. Wang, Y. Nie, Acta Crystaloogr. E65 (2009) m904;
(b) A. Castineiras, J.A. Castro, M.L. Duran, J.A. Garcia-Vazquez, A. Macias, J. Romero, A. Sousa, Polyhedron 8 (1989) 2543;
(c) B. Bhagyaraju, P.S. Rao, T. Swu, Acta Crystallogr. E68 (2012) m1523.
[3] (a) S. Yamada, L. Yamanouchi, Bull. Chem. Soc Jpn. 42 (1969) 2562;
(b) C. Alvariro, J. Romero, A. Sousa, M.L. Duran, Z. Anorg. Allg. Chem. 556 (1988) 223;
(c) R.K. Parashar, R.C. Sharma, A. Kumar, G. Moha, Inorg. Chim. Acta 151 (1988) 201;
(d) M.I. Ayad, S.A. Sallam, H.E. Mabrouk, Thermochim. Acta 189 (1991) 65.
[4] M. Enamullah, M.A. Quddus, M.R. Hasan, G. Pescitelli, R. Berardozzi, G. Makhloufi, V. Vasylyeva, C. Janiak, Dalton Trans. 45 (2016) 667.
[5] M. Enamullah, A.K.M. Royhan Uddin, G. Pescitelli, R. Berardozzi, G. Makhloufi, V. Vasylyeva, A-C. Chamayou, C. Janiak, Dalton Trans. 43 (2014) 3313.
[6] M. Enamullah, M.A. Quddus, M.R. Hasan, G. Pescitelli, R. Berardozzi, G.J. Reiß, C. Janiak, Eur. J. Inorg. Chem. (2015) 2758.
[7] M. Enamullah, G. Makhloufi, R. Ahmed, B.A. Joy, M.A. Islam, D. Padula, H. Hunter, G. Pescitelli, C. Janiak, Inorg. Chem. 55 (2016) 6449.
[8] (a) M. Enamullah, V. Vasylyeva, C. Janiak, Inorg. Chim. Acta 408 (2013) 109;
(b) M. Enamullah, M.K. Islam, J. Coord. Chem. 66 (2013) 4107.
[9] A.-C. Chamayou, G. Makhloufi, L.A. Nafie, C. Janiak, S. Lüdeke, Inorg. Chem. 54 (2015) 2193.
[10] M. Enamullah, A.K.M. Royhan Uddin, A.-C. Chamayou, C. Janiak, Z. Naturforsch. 62b (2007) 807.
[11] C. Janiak, A.-C. Chamayou, A.K.M. Royhan Uddin, M. Uddin, K.S. Hagen, M. Enamullah, Dalton Trans. (2009) 3698.
[12] M. Enamullah, A.K.M. Royhan Uddin, G. Hogarth, C. Janiak, Inorg. Chim. Acta 387 (2012) 173.
[13] M. Enamullah, J. Coord. Chem. 64 (2011) 1608.
[14] M. Enamullah, A.K.M. Royhan Uddin, G. Hogarth, J. Coord. Chem. 65 (2012) 4263.
[15] M. Enamullah, J. Coord. Chem. 65 (2012) 911.
[16] M. Enamullah, M.A. Quddus, M.A. Halim, M.K. Islam, V. Vasylyeva, C. Janiak, Inorg. Chim. Acta 427 (2015) 103.
[17] M. Enamullah, M.A. Islam, B.A. Joy, G.J. Reiss, Inorg. Chim. Acta 453 (2016) 202.
[18] M. Enamullah, M.A. Quddus, M.M. Rahman, T.E. Burrow, J. Mol. Struct. 1130 (2017) 765.
[19] B.M. Drašković, G.A. Bogdanović, M.A. Neelakantan, A.-C. Chamayou, S. Thalamuthu, Y.S. Avadhut, J. Schmedt auf der Günne, S. Banerjee, C. Janiak, Cryst. Growth Des. 10 (2010) 1665.
[20] K. Sarmah, G. Pandit, A.B. Das, B. Sarma, S. Pratihar, Cryst. Growth Des. 17 (2017) 368.
[21] (a) A.J. McKinnon, T.N. Waters, D. Hall, J. Chem. Soc. (1964) 3290;
(b) D. Hall, A.J. McKinnon, T.N. Waters, J. Chem. Soc. (1965) 425;
(c) J.A. Bevan, D.P. Graddon, J.F. McConnell, Nature (London) 199 (1963) 373;
(d) A. Elmali, Y. Elerman, I. Svoboda, H. Fuess, Z. Kristallogr. 210 (1995) 612;
(e) G.Q. Zhang, G.Q. Yang, J.S. Ma, J. Chem. Res. (2006) 19.
[22] APEX-2, APEX-2, Data Collection Program for the CCD Area-Detector System, Version 2.1-0, Bruker Analytical X-ray Systems, Madison (WI), 2006.
[23] G.M. Shekdrick, SHELXL-97 – Program for Crystal Structure Refinement, University of Göttingen, Germany, 1997.
[24] M.J. Frisch, G.W. Trucks, H.B. Schlegel, G.E. Scuseria, M.A. Robb, J.R. Cheeseman, G. Scalmani, V. Barone, B. Mennucci, G.A. Petersson, H. Nakatsuji, M. Caricato, X. Li, H.P. Hratchian, A.F. Izmaylov, J. Bloino, G. Zheng, J.L. Sonnenberg, M. Hada, M. Ehara, K. Toyota, R. Fukuda, J. Hasegawa, M. Ishida, T. Nakajima, Y. Honda, O. Kitao, H. Nakai, T. Vreven, J.A. Montgomery Jr., J.E. Peralta, F. Ogliaro, M. Bearpark, J.J. Heyd, E. Brothers, K.N. Kudin, V.N. Staroverov, R. Kobayashi, J. Normand, K. Raghavachari, A. Rendell, J.C. Burant, S.S. Iyengar, J. Tomasi, M. Cossi, N. Rega, J.M. Millam, M. Klene, J.E. Knox, J.B. Cross, V. Bakken, C. Adamo, J. Jaramillo, R. Gomperts, R.E. Stratmann, O. Yazyev, A.J. Austin, R. Cammi, C. Pomelli, J.W. Ochterski, R.L. Martin, K. Morokuma, V.G. Zakrzewski, G.A. Voth, P. Salvador, J.J. Dannenberg, S. Dapprich, A.D. Daniels, Ö. Farkas, J.B. Foresman, J.V. Ortiz, J. Cioslowski, D.J. Fox, Gaussian 09, Revision D.01, Gaussian Inc., Wallingford CT, 2009.
[25] M. Enamullah, M.K. Islam, M.A. Halim, C. Janiak, J. Mol. Struct. 1099 (2015) 154.
[26] M. Enamullah, M.K. Islam, C. Janiak, J. Mol. Struct. 1122 (2016) 331.
[27] A. Ipatov, F. Cordova, L.J. Doriol, M.E. Casida, J. Mol. Struct. (THEOCHEM) 914 (2009) 60.
[28] Q. Luo, L. Kong, C. Shen, S. Yu, Q. Lu, L. Huang, Transition Met. Chem. 18 (1993) 583.
[29] A.M. Herrera, G.V. Kalayda, J.S. Disch, J.P. Wikstrom, I.V. Korendovych, R.J. Staples, C.F. Campana, A.Y. Nazarenko, T.E. Haas, E.V. Rybak-Akimova, Dalton Trans. (2003) 4482.
[30] C. Li, Catal. Rev. Sci. Eng. 46 (2006) 419.
[31] Q.H. Xia, H.Q. Ge, C.P. Ye, Z.M. Liu, K.X. Su, Chem. Rev. 105 (2005) 1603.
[32] (a) G.J.M. Fernandez, E. Acevedo-Arauz, R. Cetina-Rosado, R.A. Toscano, N. Macías-Ruvalcaba, M. Aguilar-Martínez, Transition Met. Chem. 24 (1999) 18;
(b) G.J.M. Fernandez, O. Ruíz-Ramírez, R. Toscano, N. Macías-Ruvalcaba, M. Aguilar-Martínez, Transition Met. Chem. 25 (2000) 511.